Essential Readings in Light Metals: Cast Shop for Aluminum Production.
Edited by John F. Grandfield and Dmitry G. Eskin.

Light Metals — From *Light Metals 2003*, Paul N. Crepeau, Editor

MODELLING OF THE THERMO-PHYSICAL AND PHYSICAL PROPERTIES FOR SOLIDIFICATION OF AL-ALLOYS

N.Saunders[1], X.Li[2], A.P.Miodownik[1] and J.-P.Schillé[2]

[1]Thermotech Ltd., Surrey Technology Centre, The Surrey Research Park, Guildford GU2 7YG, U.K.
[2]Sente Software Ltd., Surrey Technology Centre, The Surrey Research Park, Guildford GU2 7YG, U.K.

Abstract

The thermo-physical and physical properties of the liquid and solid phases are critical components in casting simulations. Such properties include the fraction solid transformed, enthalpy release, thermal conductivity, volume and density, all as a function of temperature. Due to the difficulty in experimentally determining such properties at solidification temperatures, little information exists for multi-component alloys. As part of the development of a new computer program for modelling of materials properties (JMatPro) extensive work has been carried out on the development of sound, physically based models for these properties. Wide ranging results will presented for Al-based alloys, which will include more detailed information concerning the density change of the liquid that intrinsically occurs during solidification due to its change in composition.

Introduction

Casting of Al-alloys is one of the most important features of Al technology and the increasing use of process modelling software to design and optimise castings makes it important that the thermo-physical and physical properties of Al alloys are well characterised, as they are critical input for almost all types of process models. Obtaining these properties at low temperatures can be a time-consuming and expensive procedure if all relevant properties are considered. Experimental measurement becomes more problematical at high temperature, especially if the liquid phase is involved. To this end it is highly desirable to calculate thermo-physical and physical properties over the whole solidification range for as wide a range of alloys as possible.

The present paper describes a general methodology to calculate properties such as density, thermal conductivity, specific heat (C_p), solidification shrinkage etc. for multi-component alloys. The property models that are described in the present paper have also been linked to the simulation of non-equilibrium solidification based on the Scheil-Gulliver (SG) model. Hence it is possible to directly input calculated values into casting simulation packages.

The current work forms part of the development of a more generalized software package (JMatPro) for the calculation of wide ranging of materials properties [1]. A feature of the new program is that great store has been placed on using models that, as far as possible, are based on sound physical principles rather than purely statistical methods. Thus many of the shortcomings of methods such as regression analysis can be overcome. For example, the same model and model parameters are used for density calculations for all alloy types, whether it is for a commercially pure Al or a complex Ni-based superalloy.

The paper will describe the SG solidification model that directly calculates fraction solid, Cp, enthalpy and latent heat of solidification. Details concerning the creation of a molar volume database that enables a variety of properties to be calculated, such as solidification shrinkage, density, thermal expansion coefficient, will then be presented. The calculation of thermal conductivity will also be discussed. Examples of the linking of the solidification models with the physical property calculations will be made and properties during solidification will be calculated for a series of Al-alloys and the results presented. A significant advantage of the current method is that properties for each phase are calculated so fine detail can be obtained; for example the density change of the liquid during the solidification, which is governed both by an intrinsic change as the temperature is changed and also by the composition changes that accompany solidification.

Background

Solidification modelling

Recently the application of so-called 'Scheil-Gulliver' modelling via a thermodynamic modelling route has led to the ability to predict a number of critical thermo-physical properties for a variety of alloy types [2,3,4,5,6,7] during solidification. Such calculations can be computationally very fast and are currently used within solidification packages such as ProCAST [2].

For equilibrium solidification described by the lever rule and with linear liquidus and solidus lines, the composition of the solid (C_s) as a function of the fraction solid transformed (f_S) is given by

$$C_s = \frac{kC_o}{f_s(k-1)+1} \qquad .....(1)$$

where k is the partition coefficient and C_o is the composition of the original liquid alloy. This can be re-arranged to give

$$f_s = \left(\frac{1}{1-k}\right)\left(\frac{T_L - T}{T_f - T}\right) \qquad .....(2)$$

where T_L and T_f are the equilibrium liquidus and solidus temperatures. A complementary limiting case to equilibrium solidification is to assume that solute diffusion in the solid phase is small enough to be considered negligible and that diffusion in the liquid is extremely fast, fast enough to assume that diffusion is complete. In this case eq.1 can be re-written as

$$C_s = kC_o(1-f_s)^{k-1} \qquad ....(3)$$

and eq.2 as

$$f_s = 1 - \left(\frac{T_f - T}{T_f - T_L}\right)^{\left[\frac{1}{k-1}\right]} \quad .....(4)$$

The treatment above is the traditional derivation of the Scheil equation but it has quite severe restrictions when applied to multi-component alloys. It is not possible to derive this equation, using the same mathematical method, if the partition coefficient, k, is dependent on temperature and/or composition. The Scheil equation is applicable only to dendritic solidification and cannot, therefore, be applied to eutectic alloys that are common type for Al-alloys. Further it cannot be used to predict the formation of intermetallics during solidification.

Using thermodynamic modelling all of the above disadvantages can be overcome. The process that physically occurs during 'Scheil' solidification can be envisaged as follows (Fig.1). A liquid of composition C_o is cooled to a small amount below its liquidus. It precipitates out solid with a composition $C_{S,1}$ and the liquid changes its composition to $C_{L,1}$. However, on further cooling to the initial solid cannot change its composition due to lack of back diffusion and it is effectively 'isolated'. A local equilibrium is then set up where the liquid of composition $C_{L,1}$ transforms to a liquid of composition $C_{L,2}$ and a solid with composition $C_{S,2}$, which is precipitated onto the original solid with composition $C_{S,1}$. This process occurs again on cooling where the liquid of composition $C_{L,2}$ transforms to a liquid of composition $C_{L,3}$, and a solid with composition $C_{S,3}$ grows on the existing solid. This process occurs continuously during cooling and when $k<1$ leads to the solid phase becoming lean in solute in the center of the dendrite and the liquid becoming more and more enriched in solute as solidification proceeds. Eventually, the composition of the liquid will reach the eutectic composition and final solidification will occur via this reaction.

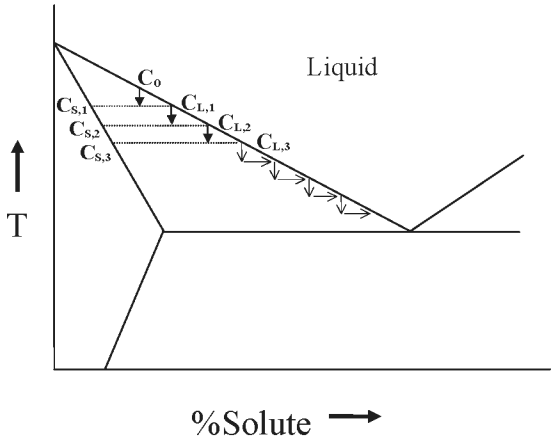

Figure 1. Schematic representation of solidification occurring under Scheil-Gulliver conditions

Any appearance of secondary phases can be easily taken into account in this approach with the assumption that no back diffusion occurs in them. Therefore, all transformations can be accounted for, including the final eutectic solidification. The approach described here is based on an isothermal step process but as the temperature step size becomes small it provides results that are almost completely equivalent to that which would be obtained from continuous cooling. A further and very significant advantage of using a thermodynamic approach is that the heat evolution during solidification is a straightforward product of the calculation. The limit to the SG simulation is that some back diffusion will take place. However, if the degree is small, good results will still be obtained and comparison of experimentally determined solidification behaviour and SG calculations for Al-alloys match very well [6,8].

The Calculation of C_p, Enthalpy and Latent Heat of Solidification.

As mentioned above, an advantage of using the CALPHAD methodology for solidification modelling is that as well as calculating the fraction solid transformed, the phases formed themselves and their amounts, heat evolution is calculated. This is critical input to casting simulation software. Figures 2 & 3 show respectively the fraction solid transformed and the enthalpy of a 356 alloy during casting.

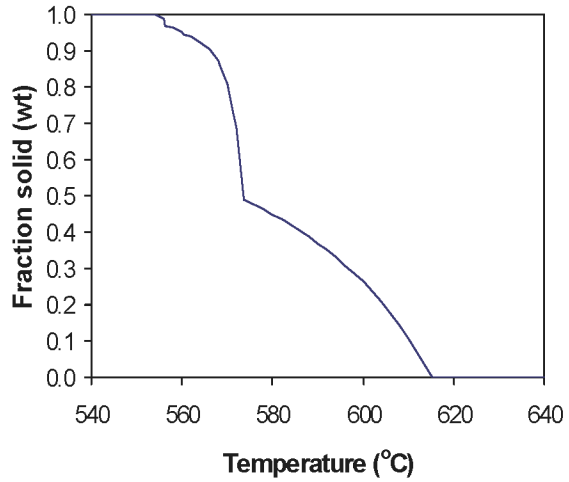

Figure 2. Calculated fraction solid vs. temperature for a 356 alloy during solidification

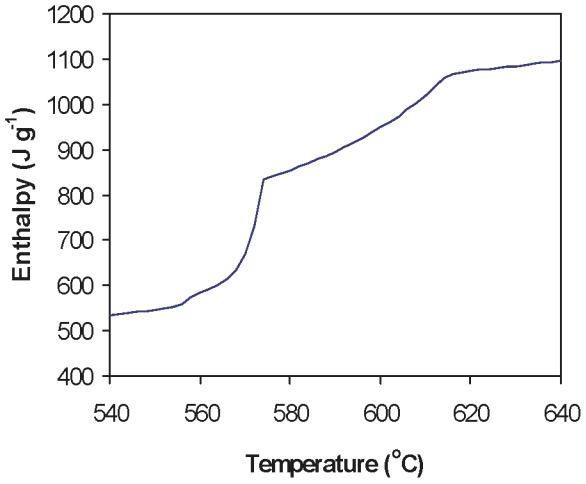

Figure 3. Calculated enthalpy vs. temperature for a 356 alloy during solidification

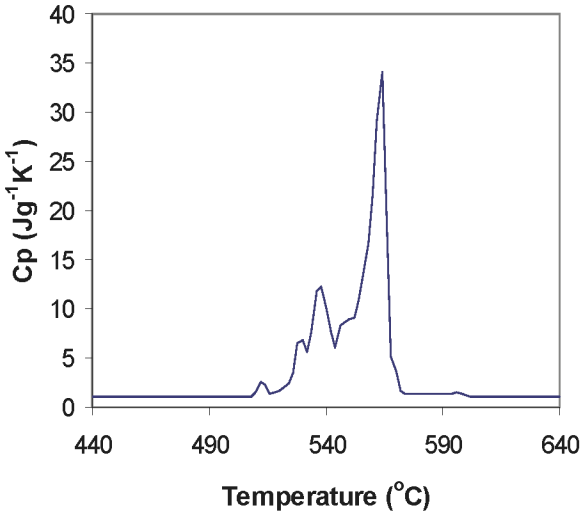

Figure 4. Cp vs. temperature calculated for a 339-1 Al-alloy during solidification

Differentiation of the enthalpy curve then provides the Cp values (Fig.4). At the completion of solidification, information concerning the solid phases formed during solidification is retained and their properties extrapolated below the solidus. This is particularly useful as, within a finite element mesh, the temperature can range from well below the solidus near the mould wall to above the liquidus in the feeders. Utilising modulus calculations, also provided by JMatPro, it is then possible to consider residual stresses in castings.

Molar Volume Calculations

A major achievement of the JMatPro development project has been the development of an extensive molar volume database that can be linked to its thermodynamic calculation capability and hence provide volume data for the phases involved in the calculation. Presently, an extensive database of parameters exists for most of the major phases in Al-, Fe-, Mg-, Ni- and Ti-alloys, which has been tested extensively in the solid state against lattice parameter measurements (both at room temperature and where available at high temperatures) and experimentally reported linear expansion data. Volume calculations are linked such that, once a thermodynamic calculation is made, the volume of the various phases that are formed can be directly calculated.

For pure aluminium both the behaviour of the liquid and solid phases can be readily modelled using linear expansion measurements combined with a molar volume calculated from lattice parameter or density measurements. The volume difference on melting is well characterised, as is the change in density of the liquid as a function of temperature [9]. Figure 5 shows the calculated molar volume of the FCC and liquid phases as a function of temperature.

The volume of the liquid and solid phases is represented by simple mixture models, similar to those used for modelling of thermodynamic excess functions in multi-component alloys [10] and further detail will be presented in another paper [11]. As well as the Al and liquid phases, extensive work has been done to characterise the properties of the intermetallic phases. This has involved validation against volumes determined from lattice parameter measurement alongside a simple and self-consistent extrapolation method for modelling their linear expansion. This method assumes that the linear expansion is an "ideal" mixture of those of the elements in the compound. This provides calculated solid state expansion coefficients in good agreement with experiment.

Little information exists on the volume of the liquid, even in binary alloys. Information is reported by the Auburn solidification design center for three commercial alloys [12] and it is possible to compare the shrinkage volume of binary Al-Si alloys [9]. Fig.6 shows the comparison with the commercial alloys and for the case of Al-Si alloys a eutectic alloy would have a shrinkage of ~3.25% while the calculation provides a value of 3.38%. The agreement is very encouraging

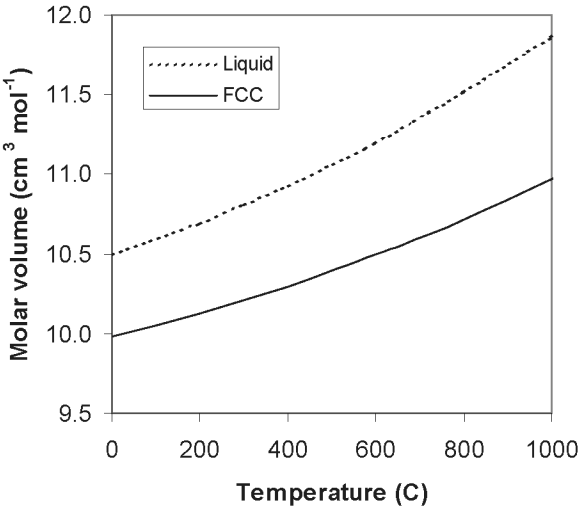

Figure 5. Calculated volumes of solid and liquid phases of Al as a function temperature.

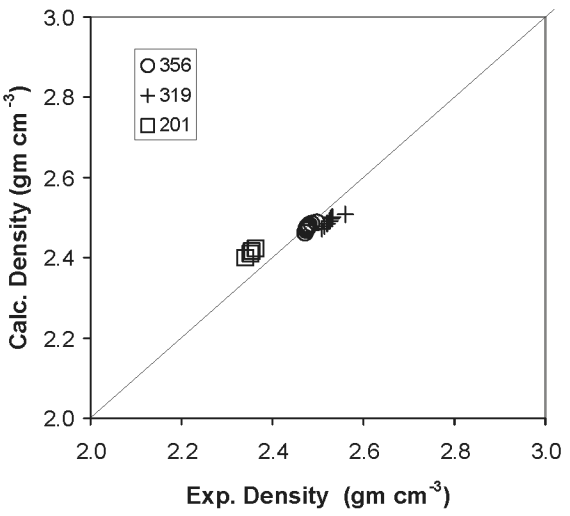

Figure 6. Comparison between calculated and reported densities of three commercial Al-alloys.

Linking the volume database to the SG calculations now means that a number of solidification properties can be calculated. Fig.7 shows the calculated shrinkage during casting of a 319 alloy. It is noted that there are two parts to the shrinkage. There is the natural shrinkage that occurs on cooling of the liquid and solid phases and also the shrinkage that occurs due to the liquid to solid transformation itself. Note that for this case, and subsequent solidification calculations, calculated properties below the solidus are also shown.

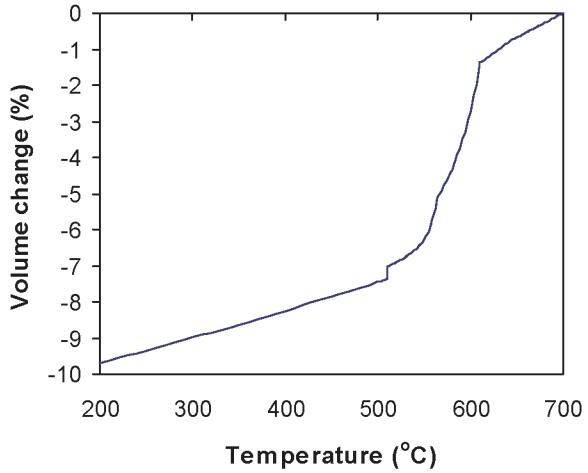

Figure 7. Calculated volume change for a 319 Al-alloy during solidification

While Fig.7 shows the overall change in volume during casting, it is straightforward to gain more detail by looking at the density change of the alloy and, in particular, the density change of the liquid. In this case we have plotted the density of the liquid in the mushy zone as well as in the fully liquid state (Fig.8).

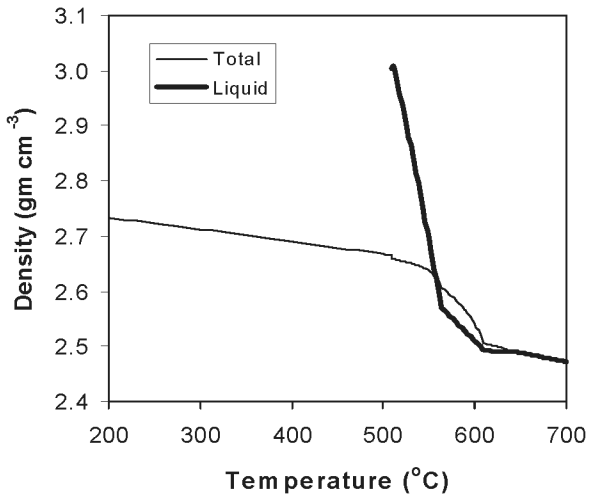

Figure 8. Calculated density change for a 319 Al-alloy during solidification.

What is apparent is that the liquid density is changing much more rapidly than the total density in the mushy zone. This can be understood by analysing the composition changes in the liquid, which show substantial enrichment of Cu as its composition changes to that of the final eutectic.

A corollary calculation made from volume calculations is to obtain the thermal coefficient of expansion and this is shown for a 339-1 alloy in Figure 9.

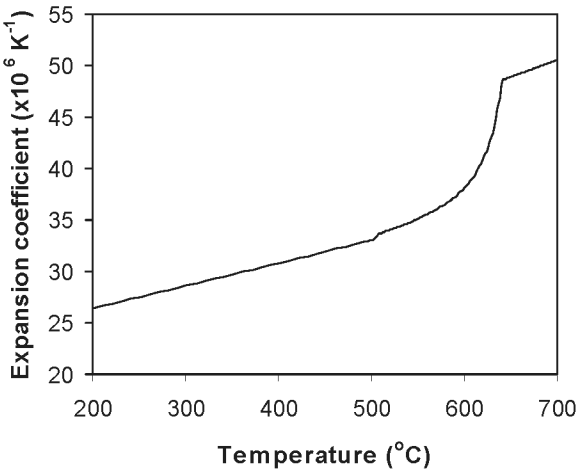

Figure 9. Calculated thermal expansion coefficient for a 339-1 Al-alloy during solidification

Thermal Conductivity Calculations

The calculation of thermal conductivity is a complex physical phenomenon. There are sharp changes on alloying in the solid state and the behaviour, in terms of mixing models, is more difficult to match. On alloying, a "bath tub" shape is often seen, where the thermal conductivity falls sharply in the dilute range and then forms a fairly flat plateau in the concentrated region [13]. Because of the lack of information concerning the thermal conductivity of binary liquid Mg-alloys alloys we cannot directly assess coefficients for alloying effects in the liquid. However, information does exist for thermal conductivity in the liquid state in pure elements and we have evaluated parameters using this information [14,15] as a first basis.

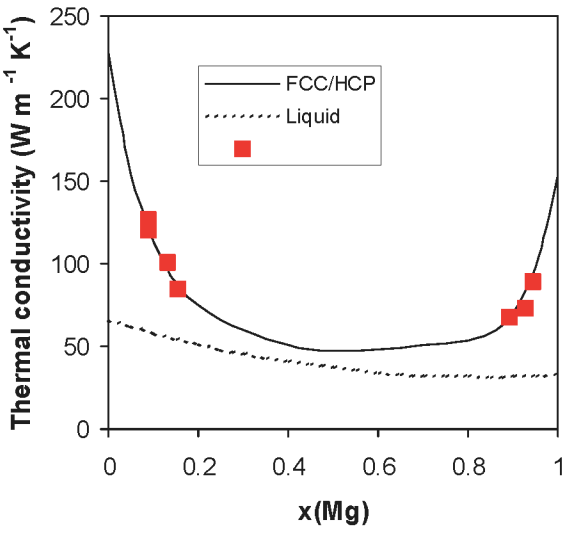

Figure 10. Calculated and experimental thermal conductivities of Al-Mg alloys at 100°C.

Fig.10 shows the calculated thermal conductivity in Al-Mg solid alloys with measured [16] thermal conductivities for the Al and Mg solid solutions shown for comparison. In this case we have assumed that the thermal conductivity of the FCC and HCP forms are the same and can be represented using one curve. A "bath tub" curve is clearly seen, but of interest is that an "ideal" extrapolation of the liquid thermal conductivity at this temperature provides thermal conductivities rather close to those in the plateau region. To obtain the usually observed result for metals, in that the thermal conductivity of the liquid should be less than that of the solid, only a small negative interaction coefficient is needed. We have invariably found this result in our assessment work and we have evaluated interaction terms based on this principle.

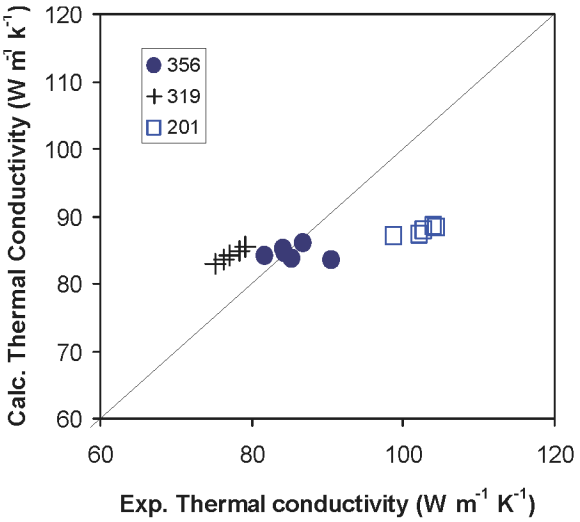

Figure 11. Comparison between calculated and reported thermal conductivities [12] of 3 commercial Al-alloys.

We have compared calculated conductivities with Al alloys reported by the Auburn solidification group [12] and the results are shown in Fig.11. The agreement is rather good for the case of 319 and 356. However, there are clear differences with 201. In this case we rather trust the calculated values because one might generally expect the thermal conductivity to decrease when alloy elements are added in dilute solution. This is the case for 201 whose main addition is ~2at% Cu. To match experiment would require a quite sharp increase in thermal conductivity on alloying and it's further noted that, in the solid state, the opposite is true – there is a very sharp drop in thermal conductivity.

Combining with the SG calculations allows the thermal conductivity to be calculated during solidification and this is shown for a 356 alloy in Figure 12. Application of the Wiedemann-Franz-Lorenz law [14] then allows electrical conductivity to be calculated (Fig.13).

Summary and Conclusions

Models have been developed for the calculation of the various thermo-physical and physical properties with the aim of providing thermo-physical and physical properties for various types of multi-component-alloys during solidification. The present paper describes how a Scheil-Gulliver solidification model has been combined with physical property calculations to provide

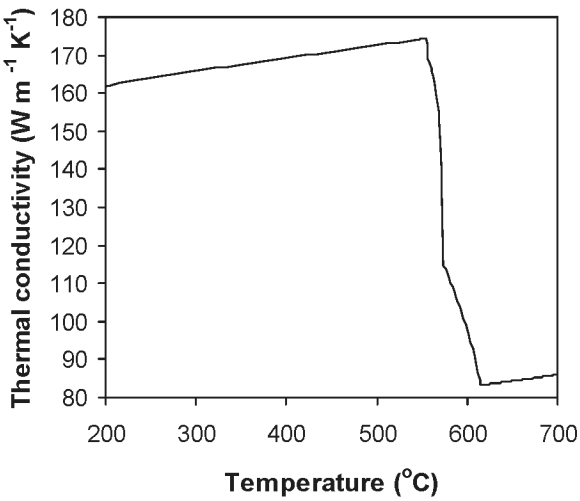

Figure 12. Calculated thermal conductivity for a 356 alloy during solidification.

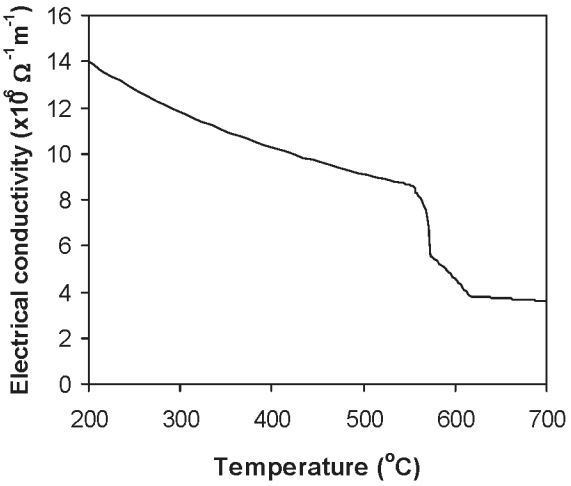

Figure 13. Calculated electrical conductivity for a 356 alloy during solidification.

calculations for fraction solid, enthalpy, Cp, thermal and electrical conductivity, density, linear expansion coefficient and volume shrinkage during solidification in a series of multi-component Al-alloys

Work is currently undergoing to model viscosity that will complete a very comprehensive set of properties of value to process modellers of all types. A further, significant advantage of the approach described here, is that it is possible to obtain important properties for each phase individually. For example, the density of the liquid phase during the solidification process is automatically calculated.

References

1. N. Saunders et al., Materials Design Approaches and Experiences, eds. J.-C.Shao et al. (Warrendale, PA: TMS: 2001), 185

2. W.J. Boettinger et al., Modelling of Casting, Welding and Advanced Solidification Processes, VII, eds. M.Cross et al., (Warrendale, PA: TMS, 1995), 649
3. N. Saunders, Superalloys 1996, eds. R.Kissinger et al. (Warrendale, PA: TMS, 1996) 115
4. B.A. Boutwell et al., Superalloys 718, 625, 706 and Various Derivatives, ed. E.A. Loria, (Warrendale, PA: TMS, 1996), 99
5. N.Saunders, Materials Science Forum, 217-222 (1996), 667
6. N.Saunders, Light Metals 1997, ed. R. Huglen (Warrendale, PA: TMS, 1997), 911
7. R.A. Harding and N. Saunders, Trans.American Foundryman's Society, 105, (1997), 451
8. N. Saunders, Solidification Processing 1997, eds. J. Beech and H.Jones (Sheffield: Univ.Sheffield, 1997), 362
9. L.F.Mondolfo "Aluminium Alloys: Structure & Properties", Butterworths, London, 1976
10. N. Saunders and A.P. Miodownik, CALPHAD – Calculation of Phase Diagrams, Pergamon Materials Series vol.1, ed. R.W. Cahn (Oxford: Elsevier Science,1998)
11. N. Saunders et al., to be presented at Modeling of Casting, Welding and Advanced Solidification Processes X, Sandestin, Florida May 25-30, 2003
12. Data downloaded from web address http://metalcasting.auburn.edu/data/data.html
13. J.B.Austin The Flow of Heat in Metals (Cleveland, OH: ASM, 1942)
14. T. Iida and R.L. Guthrie "The Physical Properties of Liquid Metals", (Oxford: Clarendon Press, 1988)
15. K.C.Mills, B.J.Monaghan and B.J.Keene, Int.Met.Rev., **41**, (1996), p209
16. Y.S. Touloukian, R.W. Powell, C.Y. Ho and P.G. Kliemens, "Thermo-physical Properties of Matter: Vol.1" (IFI Plenum Press, New York, 1970)

Essential Readings in Light Metals: Cast Shop for Aluminum Production.
Edited by John F. Grandfield and Dmitry G. Eskin.

Recommended Reading

Alexander, D.T.L., et al. Investigating the alpha transformation - a solid-state phase change of dispersed intermetallic particles from an Al-6(Fe,Mn) phase to an alpha-Al-(Fe,Mn)-Si phase (2002, pp. 771–776).

Backerud, L., and M. Johnsson. The relative importance of nucleation and growth mechanisms to control grain size in various aluminum alloys (1996, pp. 679–685).

Detomi, A.M., et al. The impact of TiCAl and TiBAl grain refiners on casthouse processing (2001, pp. 919–925).

Easton, M., D. StJohn, and E. Sweet. Reducing the cost of grain refiner additions to DC casting (2004, pp. 827–831).

Fang, Q.T., and D.A. Granger. Prediction of pore size due to rejection of hydrogen during solidification of aluminum alloys (1989, pp. 927–936).

Fortier, J.L., and C. Tremblay. Segregation effects in aluminum metal samples effect of sample mold design (1984, pp. 1373–1387).

Grandfield, J.F., C.J. Davidson, and J.A. Taylor. The columnar to equiaxed transition in horizontal direct chill cast magnesium alloy AZ91 (2001, pp. 911–916).

Hardman, A., and D. Young. Grain refining performance of TICAR master alloys in various aluminum alloy systems (1998, pp. 983–988).

Hoefs, P., et al. Development of an improved AlTiC master alloy for the grain refinement of aluminium (1997, pp. 777–784).

Kearns, M.A., and P.S. Cooper. Effects of solute interactions of grain refinement of commercial aluminium alloys (1997, pp. 655–661).

Kearns, M.A., S.R. Thistlethwaite, and P.S. Cooper. Recent advances in understanding the mechanism of aluminium grain refinement by TiBAl master alloys (1996, pp. 713–720).

Quested, T.E., and A.L. Greer. Growth-restriction effects in grain refinement of aluminium (2003, pp. 945–952).

Sannes, S., L. Arnberg, and M.C. Flemings. Orientational relationships in semi-solid Al-6.5wt% Si (1996, pp. 795–798).

Schaffer, P.L., A.K. Dahle, and J.W. Zindel. Grain refiner fade in aluminium alloys (2004, pp. 821–826).

Schneider, W.A., et al. A comparison of the family of AlTiB refiners and their ability to achieve a fully equiaxed grain structure in DC casting (2003, pp. 953–959).

Schumacher, P., and A.L. Greer. High-resolution transmission electron microscopy of grain-refining particles in amorphous aluminium alloys (1996, pp. 745–753).

Suarez, O.M., and J.H. Perepezko. Microstructural observation of active nucleants in Al-Ti-B master alloys (1992, pp. 851–859).

Vatne, H.E., and A. Håkonsen. Experimental investigations of the effect of various alloying elements on as-cast grain size of wrought Al-alloys (1999, pp. 787–792).

Whitehead, A.J., S.A. Danilak, and D.A. Granger. The development of a commercial Al-3% Ti-0.15%C grain refining master alloy (1997, pp. 785–793).

Xie, F.Y., et al. Microstructure and microsegregation in a directionally solidified quaternary Al-rich Al-Cu-Mg-Zn alloy (2001, pp. 1085–1090).